



## RESEARCH ARTICLE

### Evaluation of Healthy and Subclinical Benign Prostatic Hyperplasia Affected Intact Male Dogs Using Ultrasonography and Specific Features of Computed Tomography

Tomas Laurusevičius<sup>1,2,3\*</sup>, Sigita Kerzienė<sup>1</sup>, Nomeda Juodžiukynienė<sup>2</sup>, Jūratė Šiugždaitė<sup>2</sup>, Vaiva Jackutė<sup>1,3</sup>, Viktorija Latvis<sup>4</sup>, Jakov Šengaut<sup>4</sup>, Darius Trumbeckas<sup>5</sup> and Henrikas Žilinskas<sup>1</sup>

<sup>1</sup>Lithuanian University of Health Sciences, Veterinary Academy, Tilžės str.18, Kaunas, Lithuania; <sup>2</sup>Department of Veterinary Pathobiology, Faculty of Veterinary Medicine, Veterinary Academy, Lithuanian University of Health Sciences, Tilžės str.18, Kaunas, Lithuania; <sup>3</sup>Kaunas Veterinary Practice, Veiverių str. 176a-2, Kaunas, Lithuania; <sup>4</sup>Jakovo Veterinary Centre, Gerosios Vilties str. 1, Vilnius, Lithuania; <sup>5</sup>Lithuanian University of Health Sciences, Urology Clinic, Eivenių str.2, Kaunas, Lithuania

\*Corresponding author: reprovetas@gmail.com

#### ARTICLE HISTORY (23-220)

Received: June 3, 2023  
Revised: August 22, 2023  
Accepted: August 26, 2023  
Published online: September 05, 2023

#### Key words:

Benign prostatic hyperplasia  
Intact male dogs  
Computed tomography  
Ultrasonography  
Prostate gland evaluation

#### ABSTRACT

Spontaneous benign prostatic hyperplasia (BPH) is common in aged intact male dogs; the condition is often without clinical signs. While ultrasonography is commonly used for the evaluation of health status of prostate gland, computed tomography (CT) offers advanced imaging capabilities. The latter technique allows for comprehensive investigation of the target organs, with possible incidental findings in other organs. This study aimed to evaluate the prostate gland in BPH-affected and healthy intact male dogs using ultrasonography and various CT assessment techniques. This study involved 52 intact male dogs of various breeds, ages, and weights. These dogs were divided into two study groups based on the cytological findings of the prostate gland tissue; healthy group (n=24) and a group with confirmed subclinical BPH (n=28). Animals of both groups were examined using ultrasonography and CT features to assess the health status of prostate gland. Results revealed that the length, width, height and volume of prostate gland were significantly higher in BPH-affected group than the healthy group ( $p<0.001$ ). Similarly, asymmetry and heterogeneity of the gland was observed in higher %age of BPH-affected dogs than the healthy ones ( $p<0.001$ ). BPH-affected dogs also exhibited lower contrast attenuation values and higher ratios of prostate gland dimensions to the 6th lumbar vertebra compared to healthy dogs. Additionally, ratios of prostate gland width and height to pelvic inlet dimensions were higher in BPH group ( $p<0.001$ ). In conclusion, the study shows that utilizing multiple CT imaging method, including the partial pelvimetry technique, offers both reliability for advanced imaging of the prostate gland and serves as a diagnostic tool for BPH diagnosis in dogs.

**To Cite This Article:** Laurusevičius T, Juodžiukynienė N, Šiugždaitė J, Kerzienė S, Latvis V, Šengaut J, Jackutė V, Trumbeckas D and Žilinskas H, 2023. Evaluation of healthy and subclinical benign prostatic hyperplasia affected intact male dogs using ultrasonography and specific features of computed tomography. Pak Vet J, 43(4): 764-770. <http://dx.doi.org/10.29261/pakvetj/2023.079>

#### INTRODUCTION

Benign prostatic hyperplasia (BPH) is a spontaneous and age-related para-physiological condition that affects intact male dogs (Socha *et al.*, 2018). This condition is characterized by the enlargement of the prostate gland and has been associated with oxidative stress and a decrease in antioxidant defense, potentially leading to negative effects on male reproductive ability and semen quality (Flores *et al.*, 2017). In its later stages, BPH can have broader implications for the overall health of the male dog, with the manifestation of clinical symptoms including tenesmus,

diarrhea, dysuria, hematuria, pain and lameness in the hind limbs (Pasikowska *et al.*, 2015). However, in many cases the disease remains asymptomatic in its early stages, presenting a challenge for owners and veterinarians in making timely diagnosis.

The use of diagnostic imaging tools is considered the most effective approach in veterinary medicine for evaluating the health status of the prostate gland (Alonge *et al.*, 2018; Mantziaras, 2020). Assessment of the prostate by transrectal digital palpation is performed by the veterinarian in intact adult male dogs for routine screening (Mukaratirwa and Chitura, 2007). However, since rectal

palpation has limited value, diagnostic imaging tools are frequently employed for the evaluation of the prostate gland, with ultrasonography being a commonly used technique (Lévy *et al.*, 2014). Nevertheless, the effectiveness of ultrasonography heavily relies on the experience of the operator, not only in terms of image interpretation but also in the technical aspects of the procedure. The precise identification of prostate margins, particularly the caudal contour, and selecting optimal imaging planes for ultrasonographic measurements have proven challenging (Leroy *et al.*, 2013). The presence of penis and location of prostate gland in the pelvic cavity can make it difficult to position the probe in a transverse plane (Atalan *et al.*, 1999a; Leroy *et al.*, 2013). Additionally, in some cases, ultrasonography can lead to a false diagnosis of early stages of clinical BPH (Lévy *et al.*, 2014). This issue can be overcome by using more standardized imaging techniques, such as computed tomography (CT). This has been recognized as a reliable and effective technique for the detailed examination of the reproductive organs, including the prostate gland (Mantziaras, 2020). Undeniably, CT offers many advantages over ultrasonography for evaluating the prostate gland, including detailed visualization, better tissue differentiation, three-dimensional imaging and assessment of distant metastases. In addition, CT provides better visibility of the boundaries of the prostate gland, any lesions present, its location, and the surrounding tissues compared to ultrasonographic imaging (Salonen *et al.*, 2022). Moreover, contrast-enhanced CT permits the assessment of parenchymal and vascular alterations in the target organ, providing valuable insights into the nature of the disease (Klansnoh *et al.*, 2018). Also, with the wide availability of CT and the increasing familiarity of veterinary practitioners, pet owners prefer CT scans over ultrasonography for their pets (Kuhnt *et al.*, 2020; Greco *et al.*, 2023).

Incidental findings in the reproductive tract are of particular interest during CT examinations. These unexpected discoveries, known as "incidentalomas," have the potential to reveal various unrelated diseases, including alterations in the prostate gland, when they are unexpectedly encountered during CT imaging of the abdominal or pelvic regions (Caspanello *et al.*, 2023).

The present study focuses on utilizing CT imaging to explore different aspects of the canine prostate gland in healthy intact male dogs and those affected by subclinical BPH. The primary objective was to investigate various CT assessment techniques for evaluating the prostate gland in animals of these two groups, proposing a novel diagnostic approach to improve the detection of early stages of BPH.

## MATERIALS AND METHODS

**Ethics:** The research was performed in accordance with Law of the Republic of Lithuania No. VIII-500 on the Care, Welfare and Use of Animals, dated November 06, 1997 (Valstybės žinios (Official Gazette) No. 108, 28/11/1997) and orders of the State Veterinary Service of the Republic of Lithuania on Breeding, Care and Transportation of Laboratory Animals (No. 4-361, 31/12/1998) and on Use of Laboratory Animals for Scientific Tests (No. 4-16,

18/01/1999). The approval number of the study was PK No.012856.

**Experimental animals:** This study was conducted from August 2019 to January 2023 at a private veterinary clinic in Vilnius, Lithuania. A total of 52 male dogs of different breeds, aged 3 to 10 years (average 5.7 years), with body weight ranging from 25 to 50kg (average 36.5kg) were included in the study. Dogs were presented to the clinic for CT examination of abdominal and pelvic regions. All animals in the study showed no clinical signs and had no past medical history related to reproductive tract diseases. Clinical tests were performed that included prostate gland palpation and standard laboratory tests such as urinalysis, blood morphology and biochemistry analyses. All parameters were in normal ranges. Dogs were divided into two groups (BPH-affected and healthy) based on results of prostate gland wash cytological examination, as described below. BPH-affected group consisted of 28 dogs, whereas healthy dogs group had 24 intact male dogs.

**Ultrasonography and prostate gland wash:** Ultrasound evaluations were conducted on all study dogs prior to administering anaesthesia for computed tomography (CT). During the ultrasound examination, the shape and echogenicity of the prostate gland were assessed according to the guidelines for prostate gland evaluation established by Russo *et al.* (2012). Following the ultrasound examination, prostatic wash was performed after inducing anaesthesia, and then the animals underwent CT scans. For prostate gland wash, the urinary bladder was emptied using urinary catheter, and was then rinsed multiple times with saline before being emptied again. A urinary catheter was then inserted into the prostatic urethra, the prostate was vigorously massaged through the rectum, and normal saline (10mL) was slowly injected through the catheter. Continuous aspiration was applied as the catheter was advanced through the prostatic urethra into the urinary bladder. The fluid obtained was collected in a syringe and subjected to cytological examination (Smith, 2008). Diagnosis of BPH was based on the presence of large groups of epithelial cells with typical columnar or polygonal appearance, low nuclear/cytoplasm ratio, and uniform round nuclei with small nucleoli and fine granular chromatin patterns, as described by Teske (2009).

**Computed tomography:** The computed tomography was performed under general anaesthesia. Animals of both groups were scanned in dorsal recumbency using radiolucent positioning aids to maintain stable positioning. For premedication, medetomidine hydrochloride (Cepetor 1.0mg/ml) at 10µg/kg body weight was given intravenously. Anaesthesia was induced with propofol (Propoven 10.0mg/ml) at 2-4mg/kg. For maintenance, all dogs were intubated with tracheal tube and inhalation anaesthesia with isoflurane gas was used.

The CT scans were performed using a helical 2 slice CT scanner (Somatom Spirit 2, Siemens, Germany), using 130kV Voltage, 100mAs current and 3-5mm slice thickness (reconstructions of 1.5-2.5mm). Raw data was reconstructed in soft tissue and bone algorithms. Pre- and post-contrast studies were performed, using iohexol (Omnipaque 350mg/ml, GE Healthcare AS, Norway) as

contrast media at 600mg/kg (I/V). Prostatic attenuation values were quantified within specific regions of interest (ROI) and expressed in Hounsfield Units (HU). All CT scan images were obtained in DICOM format and analysed using OsiriX software (Pixmeo SARL, Bernex, Switzerland).

Prostatic length was measured on a dorsal plane, while width and height were measured on the transverse plane. The length of the sixth lumbar vertebral body (L6) was determined by measuring it in both sagittal and dorsal plane images. A median value of these measurements was then calculated and document (Fig. 1). The ratios of prostatic length (rL6), width (rW6) and height (rH6) to the length of the L6 body were measured according to the study published by Pasikowska *et al.* (2015).

The pelvic inlet diameter was measured using sagittal and transverse images. Then the ratios of the width and height of the prostate gland with width and height of pelvic inlet were measured, using the formulas ppW and ppH, respectively. To visualize the pelvic inlet and the prostate gland affected by BPH, specialized software for 3D imaging tools was used for reconstruction. All measurements and the complete image are presented in Fig. 2.

The special features of the OsiriX (Pixmeo SARL, Bernex, Switzerland) workstation were used to calculate the prostate gland volume. Initially, the region of interest (ROI) was manually drawn using freehand tools. Subsequently, the software tools automatically calculated the prostatic volume based on this drawn ROI. Additionally, we employed 3D reconstructions, allowing the software to automatically reconstruct the prostate gland volume for more comprehensive analysis.

**Statistical analysis:** Data analysis was conducted using IBM SPSS Statistics 29.0.0.0 (241). The normality of the data was assessed using the Kolmogorov-Smirnov test. The Chi-square test was used to evaluate changes in the shape and echogenicity of the prostate gland, while other data were compared through Independent-Samples T test. Confidence intervals (CI 95%) for proportions were determined using the Wilson method (Wilson, 1927). Pearson's linear correlation coefficients and regression analysis were employed to examine the relationships between the investigated traits. Receiver operating analysis (ROC) was conducted to establish a cutoff value for prostate gland volume, yielding a threshold for BPH occurrence with an Area Under the Curve (AUC) of 0.923, sensitivity of 78.6%, and specificity of 95.8% ( $p < 0.001$ ). The ROC analysis graph showcases had the ability to differentiate healthy dogs from those with asymptomatic BPH using external characteristics. The probability level of  $p < 0.05$  was considered statistically significant.

## RESULTS

**Evaluation of the prostate gland with ultrasound:** In the healthy dogs group, a total of 7 out of 24 investigated prostate glands (29.2%, 95% CI=14.9-49.2%) exhibited asymmetric shape, suggesting that the majority of prostate glands in this group tended to display a symmetrical configuration. Conversely, in the BPH-affected group, 24 out of 28 prostate glands (85.7%, 95% CI = 68.5-94.3%)

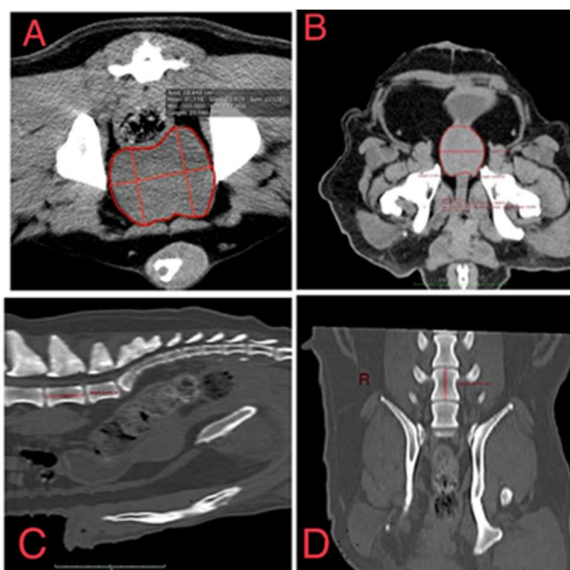


**Fig. 1:** Computed tomography images of the prostate gland and L6 vertebra. A) prostate gland, transverse plane, soft tissue algorithm. Red lines indicate measurements of prostate gland height, width and circle area; B) prostate gland, dorsal plane, soft tissue algorithm. Red lines indicate measurements of prostatic length and circle area; C) L6 vertebra, sagittal plane, bone algorithm; red line represents the length of the vertebral body. D) L6 vertebra, dorsal plane, bone algorithm; red line represents the length of the vertebral body.



**Fig. 2:** 3D image of the BPH-affected prostate gland and the pelvic bones. The prostate gland (red organ) can be appreciated in transverse projection. The A line represents the distance between closest bony point of the 2<sup>nd</sup> sacral segment and the pubic symphysis. The B line represents the closest distance between the central points of left and right acetabulum. C line shows the width of the prostate gland. D1 and D2 lines represent the height of the left and right prostatic lobes, respectively.

demonstrated asymmetric lobes, indicating a significantly higher occurrence of asymmetry in this group compared to the healthy dogs' group (Fig. 3). The proportion of asymmetric prostates was found to be substantially elevated (2.9 times) in the BPH group, with statistical significance ( $p < 0.001$ ), indicating a strong association between BPH and asymmetrical prostate gland morphology.

**Table 1:** Mean ( $\pm$ SD) values of prostate gland length, width, height and volume in dogs of two study groups.

Study groups	Prostatic length (cm)	Prostatic width (cm)	Prostatic height (cm)	Prostatic volume (cm <sup>3</sup> )
BPH-affected	5.21 $\pm$ 0.27 <sup>a</sup>	5.20 $\pm$ 0.22 <sup>a</sup>	4.45 $\pm$ 0.15 <sup>a</sup>	74.66 $\pm$ 8.02 <sup>a</sup>
Healthy	3.43 $\pm$ 0.11 <sup>b</sup>	3.65 $\pm$ 0.19 <sup>b</sup>	3.49 $\pm$ 0.14 <sup>b</sup>	24.23 $\pm$ 2.5 <sup>b</sup>

Values with different letters within a column differ significantly from each other ( $p < 0.001$ ).

**Table 2:** The parameters of Receiver Operating Characteristics (ROC) analysis.

Parameter	Prostatic length (cm)	Prostatic width (cm)	Prostatic height (cm)	Prostatic volume (cm <sup>3</sup> )
Cutoff value	4.570	4.265	3.950	46.186
Sensitivity	0.679	0.857	0.786	0.786
Specificity	1.000	0.708	0.792	0.958
AUC area	0.875	0.855	0.815	0.923
Significance of the model	$p < 0.001$	$p < 0.001$	$p < 0.001$	$p < 0.001$

Furthermore, in the BPH group, 18 out of 28 dogs (64.3%, 95% CI=45.8-79.3%) exhibited heterogeneous prostates, displaying variations in tissue composition and structural features. In contrast, only 4 out of 24 dogs in the healthy dogs' group (16.7%, 95% CI=6.7- 35.9%) showed heterogeneous prostates, indicating a significantly lower prevalence of heterogeneity in the healthy group (Fig. 3). The proportion of heterogeneous prostates was found to be significantly higher in the BPH group compared to the healthy group ( $p < 0.001$ ).

**Prostatic dimensions and volume as assessed by computed tomography:** This study demonstrated a significant increase in prostate gland volume and dimensions (length, width, and height) in the BPH-affected male dogs group compared to the healthy dogs group ( $p < 0.001$ ; Table 1). In the BPH group, the prostatic length, width, height and volume were 1.5, 1.4, 1.3 and 3.1 times higher, respectively, compared to the healthy group ( $p < 0.001$ ).

The results of the Receiver Operating Characteristic (ROC) analysis, presented in Fig. 4 and Table 2, demonstrate that all dimensions of the prostate gland allowed for a differentiation between healthy dogs and those affected by BPH. When volume of the prostate was equal to or exceeded 46.186cm<sup>3</sup>, the probability of classifying it as BPH-affected was 92.3% ( $p < 0.001$ ). Furthermore, the length, width and height of the prostate also showed significant discriminatory capability in distinguishing healthy dogs from those with BPH. The probability of correct classification was slightly lower compared to using volume, with values of 87.5% for length, 85.5% for width and 81.5% for height ( $p < 0.001$ ).

**Prostatic measurements ratio to L6:** In the present study, male dogs with confirmed BPH exhibited significantly higher mean ( $\pm$ SD) values of rL6, rW6 and rH6, representing the prostatic length, width and height ratio to the length of the 6th lumbar vertebra body, respectively, compared to the healthy dogs group ( $p < 0.001$ ; Table 3). Specifically, the ratio of rW6 was increased by 43.6% ( $p < 0.001$ ), that of rH6 by 30.1% ( $p < 0.001$ ) and for rL6 by 48.1% ( $p < 0.001$ ).

**Prostatic measurements ratio to pelvic inlet:** In the present study, mean ppW (ratio between pelvic inlet width and prostate gland width) and ppH (ratio between pelvic inlet height and prostate gland height) were significantly higher in BPH-affected group compared to the healthy dogs group (Table 4). Furthermore, the study recorded a significant negative correlation between the age of all dogs

**Table 3:** Mean ( $\pm$ SD) values of ratios between prostate gland dimensions and sixth lumbar vertebra body length in both study groups.

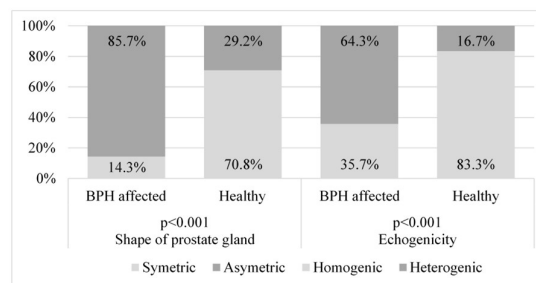
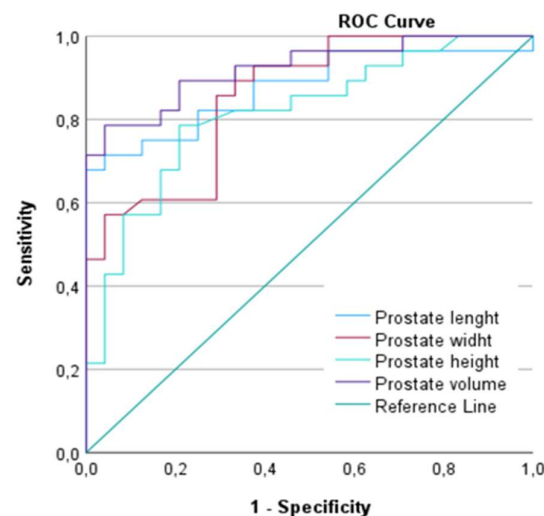
Study groups	rW6	rH6	rL6
BPH-affected	1.58 $\pm$ 0.44 <sup>a</sup>	1.34 $\pm$ 0.21 <sup>a</sup>	1.57 $\pm$ 0.48 <sup>a</sup>
Healthy	1.10 $\pm$ 0.29 <sup>b</sup>	1.03 $\pm$ 0.26 <sup>b</sup>	1.06 $\pm$ 0.16 <sup>b</sup>

Values with different letters within a column differ significantly from each other ( $p < 0.001$ ).

**Table 4:** The mean ( $\pm$ SD) values of ratios of prostate gland width and height with pelvic inlet width and height measurements in BPH-affected and healthy dogs groups.

Study groups	ppW	ppH
BPH-affected	1.02 $\pm$ 0.27 <sup>a</sup>	0.71 $\pm$ 0.13 <sup>a</sup>
Healthy	0.74 $\pm$ 0.19 <sup>b</sup>	0.57 $\pm$ 0.12 <sup>b</sup>

Values with different letters within a column differ significantly from each other ( $p < 0.001$ ).

**Fig. 3:** Shape and echogenicity of the prostate gland in both study groups. Differences in %age of asymmetric and heterogenic glands between BPH-affected and healthy dogs are significant ( $p < 0.001$ ).**Fig. 4:** Receiver Operating Characteristics (ROC) curves of prostate gland dimensions (length, width and height) and prostatic volume.

included in the study and the ratios of pelvic inlet width and width of the prostate gland ( $r = -0.586$ ,  $p < 0.001$ ). Similarly,

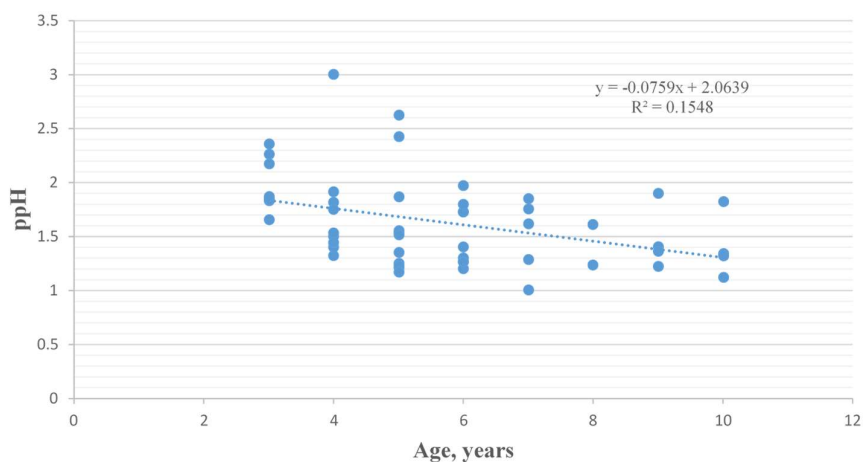


**Fig. 5:** Graphical diagram of scatter plot that represents the relationship of pelvic inlet height and prostate gland height (ppH) and the age of 52 intact male dogs ( $p < 0.05$ ).

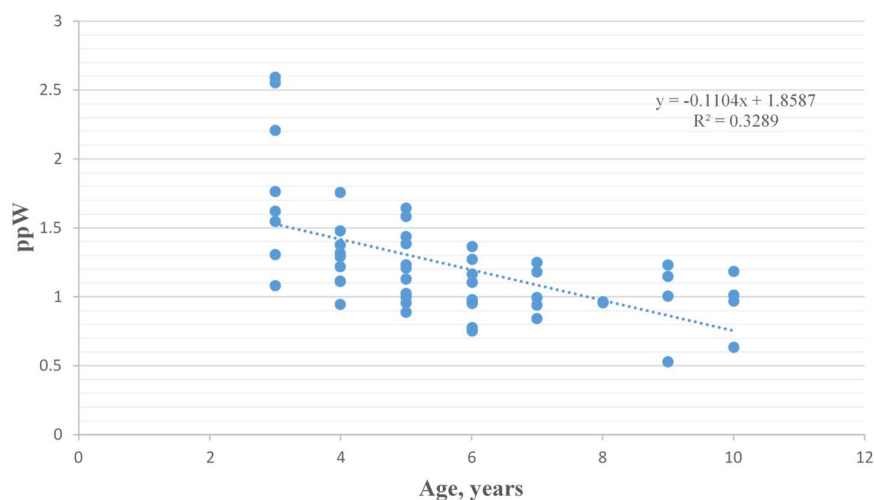


**Fig. 6:** Graphical diagram of scatter plot that represents the relationship of pelvic inlet width and prostate gland width (ppW) and the age of 52 intact male dogs ( $p < 0.05$ ).

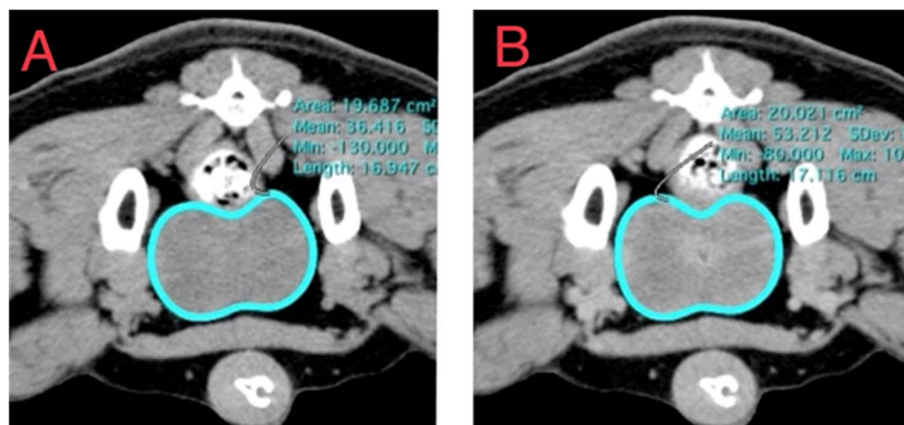


**Fig. 7:** Contrast phases of prostate gland. Region of interest (mint color line) was drawn using freehand software feature. A: Pre-contrast phase. B: Post-contrast phase.

**Table 5:** Mean ( $\pm$ SD) Hounsfield Unit (HU) values of different contrast phases in prostate gland in BPH-affected and healthy dogs groups.

Study groups	Pre-contrast	Post-contrast
BPH group	64.18 $\pm$ 9.98	92.61 $\pm$ 1.83 <sup>a</sup>
Healthy group	67.83 $\pm$ 3.56	95.42 $\pm$ 2.34 <sup>b</sup>

Values with different letters within a column differ significantly from each other ( $p < 0.001$ ).

negative correlation was found between pelvic inlet height and prostate gland height ( $r = -0.489$ ,  $p < 0.001$ ), as has been shown in Fig. 5 and 6.

**Attenuation values in pre- and post-contrast phases:** The attenuation values obtained from the pre- and post-

contrast studies underwent comprehensive analysis in both study groups. In the pre-contrast studies, the statistical analysis yielded intriguing results, revealing non-significant difference between dogs of the two groups. However, in stark contrast, the post-contrast phase unveiled significant differences between the two study groups, mean HU value was higher in healthy dogs compared to BPH group ( $p < 0.001$ ), signifying that the post-contrast attenuation values exhibited significant variations (Table 5). Moreover, to provide visual of the prostate gland in different contrast phases, illustrative images depicting pre- and post-contrast studies have been shown in Fig. 7.

## DISCUSSION

Benign prostatic hyperplasia (BPH) is a prevalent sex gland disease in aged male dogs, affecting more than 80% of males over 5 years old (Socha *et al.*, 2018). This disease may not cause noticeable symptoms at early stages, but when the prostate gland enlarges (prostatomegaly), certain signs like tenesmus, diarrhea, or difficulty in urinating (dysuria) may appear (Zelli *et al.*, 2013). Early diagnosis and management of BPH are essential, even in the absence of overt clinical signs, as approximately 95% of dogs with BPH do not show clinical signs of prostatic disease at 9 years of age (Memon, 2007). In our study, we focused on investigating the prostate gland in two groups of dogs: one group was affected with BPH but without clinical symptoms, and another group consisting of clinically healthy dogs.

Ultrasonographic examination of experimental dogs revealed that BPH was associated with a higher occurrence of asymmetric and heterogeneous prostates compared to healthy dogs, indicating distinct morphological differences between the two groups. This highlights the potential utility of prostate gland asymmetry and heterogeneity as indicators of BPH in male dogs. Similarly, Lévy *et al.* (2014) also focused on the appearance of the prostate gland in BPH-affected dogs. According to these workers, prostate gland changes in BPH-affected intact male dogs are often characterized by asymmetrical shapes of the lobes and hyperechogenic patterns in the parenchyma. It is interesting to note that in the present study 29.2% of healthy dogs also showed asymmetric glands. Moreover, 16.7% of healthy glands also had heterogenic prostate glands.

The enlargement of the prostate gland in BPH-affected dogs was evident through CT scanning in the present study, with a significant increase in length, width, height and volume of the gland compared to healthy dogs. Salonen *et al.* (2022) also emphasized the usefulness of CT imaging in assessing prostate gland volume in dogs with BPH and in healthy individuals. The observed significant differences in prostatic volume between BPH-affected and healthy dogs provide valuable insights into the impact of BPH on prostate gland enlargement. Ruel *et al.* (1998) and Atalan *et al.* (1999b) investigated prostate glands of healthy intact male dogs of various breeds, ages and weights, and reported average prostate gland volume ranging from 12 to 30cm<sup>3</sup>. However, only healthy dogs were included in both these studies. In this regard, we used ROC analysis to distinguish a healthy prostate gland from one affected by BPH. Additionally, based on our results, we proposed threshold of prostatic volume for suspicions of BPH. This threshold of 46cm<sup>3</sup> could serve as a useful indicator for suspecting BPH in intact male dogs over 3 years of age and medium to large in size. However, the established threshold should be carefully considered since prostate gland size can vary significantly among individual dogs and is influenced by multiple factors (Niżański *et al.*, 2020). Therefore, while the threshold can provide valuable guidance, it is essential for veterinarians to take into account these individual variations when assessing the health status of the prostate gland in male dogs without any clinical signs.

Pasikowska *et al.* (2015) examined the prostate glands of 40 intact male dogs with varying age, breed, and weight using computed tomography. These authors categorized

the dogs into two groups: Group A comprised 20 healthy dogs without clinical signs, while Group B included 20 dogs diagnosed with BPH and exhibiting clinical symptoms associated with the disease. These workers found that prostatic hyperplasia was associated with higher ratios between L6 body length and prostatic length (rL6), width (rW6) and height (rH6) in the BPH-affected dogs compared to the healthy dogs ( $p < 0.001$ ). Our study also indicated significantly higher mean ratios between rL6, rW6 and rH6 in the BPH-affected dogs compared to the healthy dogs. These findings emphasize the need to consider various factors when interpreting prostate gland measurements and their potential significance in diagnosing BPH in male dogs, especially in cases where the prostate gland and L6 can be observed during unrelated scanning.

In our research we also introduced a novel approach of applying partial pelvimetry to evaluate BPH-affected and healthy prostate glands. Pelvimetry is commonly used in human medicine to evaluate pelvic bone dimensions in women, particularly for assessing cephalopelvic disproportion and the risk of dystocia during childbirth (Nishikawa *et al.*, 2023). It has also been used in veterinary medicine for similar purposes (Eneroth *et al.*, 1999). Atalan *et al.* (1999b) conducted measurements of the pubic brim-sacral promontory distance and compared it with the measurements of prostate gland depth and length. This was one of the first attempts to use pelvic bones and explore the relationship between these measurements in order to assess potential correlations, providing valuable insights into the anatomical associations between the pubic brim-sacral promontory distance and the dimensions of the prostate gland. However, according to Choi *et al.* (2014), this method is subjective and inaccurate due to observer variability. Considering this limitation, we proceeded to evaluate the pelvic inlet and the prostate gland to understand the variability of the ratios between the measurements of both structures in BPH-affected and healthy dogs. By utilizing pelvic inlet measurements and comparing them with prostate gland dimensions, we tried to assess the potential association between these structures in male dogs. Our results showed that the higher ratios between pelvic inlet width and prostate gland width, as well as pelvic inlet height and prostate gland height, in BPH-affected dogs compared to healthy dogs, suggest a potential association between prostatomegaly and pelvic inlet dimensions.

Furthermore, results of this study revealed a significant negative correlation between the age of all dogs included in the study, irrespective of the health status of the prostate gland, and the ratios of ppH and ppW. This suggests that as dogs become aged, the ratios of pelvic inlet dimensions to prostate gland dimensions tend to decrease, indicating possible age-related changes in the relationship between pelvic inlet and prostate gland. One possible explanation for this observation is that as dogs become aged, the prostate gland may develop spontaneous hypertrophy, leading to changes in the measured ratios. Nonetheless, our investigation serves as an initial model for exploring the relationship between partial pelvimetry and prostatomegaly in male dogs. The study shows that this novel evaluation approach, using non-related CT imaging of the prostate gland and pelvic inlet, allows practitioners

to effectively assess potential suspicions for early stages of BPH.

Regarding contrast-enhanced CT imaging, our results revealed that the post-contrast phase significantly decreased the Hounsfield Unit (HU) values in BPH-affected dogs compared to healthy dogs. However, there was no statistically significant difference in HU values between dogs of two groups during the pre-contrast phase. According to Pasikowska *et al.* (2015), dogs diagnosed with BPH showed mean ( $\pm$ SD) attenuation values of  $56\pm 4.39$ HU in the pre-contrast phase and  $84\pm 8.03$ HU in the post-contrast phase. Similarly, our study also showed increased attenuation from  $64.18\pm 9.98$ HU in pre-contrast phase to  $92.61\pm 1.83$ HU during post-contrast phase. These results support the notion that post-contrast attenuation values could serve as a distinguishing factor between BPH-affected and healthy dogs. The observed contrast enhancement patterns in the prostate gland may indicate vascular and tissue changes associated with BPH, further emphasizing the potential diagnostic relevance of this evaluation approach.

**Conclusions:** This study demonstrated the effectiveness of CT in assessing the prostate gland using multiple techniques. There were significant differences in the volume, contrast phases, and size measurements between healthy and diseased glands, with particular relevance to diagnosing benign prostatic hyperplasia (BPH). Notably, attenuation values proved valuable in determining presence of BPH. Additionally, measurements of the sixth lumbar vertebra and prostate gland dimensions exhibited significant differences between healthy and BPH-affected glands. Moreover, partial pelvimetry also yielded promising results in differentiating between BPH-affected and healthy male dogs. Overall, this study highlights the utility of diverse CT techniques in accurately evaluating the prostate gland and determining the need for invasive diagnostics in suspected cases of BPH. These findings enhance diagnostic capabilities and aid in decision-making for the management of BPH.

**Acknowledgement:** This study was partially funded by Lithuanian University of Health Sciences (A. Mickevičiaus g. 9, 44307 Kaunas, Lithuania) scientific funds (grant number: V-786).

**Authors' contribution:** The experiment was conducted by LT, JV and ŠJ. The materials were managed by ŠJ. Prostate gland sample collections and CT examinations were performed by LV, while JN carried out the cytological examinations. Statistical analysis was performed by KS. The manuscript was written by TL and reviewed by TD and ZH.

## REFERENCES

- Alonge S, Melandri M, Leoci R, *et al.*, 2018. Canine prostate specific esterase (CPSE) as a useful biomarker in preventive screening programme of canine prostate: CPSE threshold value assessment and its correlation with ultrasonographic prostatic abnormalities in asymptomatic dogs. *Reprod Domest Anim* 53(2):359–64.
- Atalan G, Barr FJ and Holt PE, 1999a. Comparison of ultrasonographic and radiographic measurements of canine prostate dimensions. *Vet Radiol Ultrasound* 40(4):408–12.
- Atalan G, Holt PE and Barr FJ, 1999b. Ultrasonographic estimation of prostate size in normal dogs and relationship to body weight and age. *J Small Anim Pract* 40(3): 119–22.
- Caspanello T, Masucci M, Iannelli D, *et al.*, 2023. Prevalence and features of incidental findings in veterinary computed tomography: A single-center six-years experience. *Animals* 13:591; doi: 10.3390/ani13040591.
- Choi JY, Choi SY, Lee KJ *et al.*, 2014. Volumetric estimation of the prostate gland using computed tomography in normal Beagle dogs. *J Vet Clin* 31(3): 175–79.
- Eneroth A, Linde-Forsberg C, Uhlhorn M, *et al.*, 1999. Radiographic pelvimetry for assessment of dystocia in bitches: A clinical study in two terrier breeds. *J Small Anim Pract* 40(6):257–64.
- Flores RB, Angrimani DSR, Rui BR, *et al.*, 2017. The influence of benign prostatic hyperplasia on sperm morphological features and sperm DNA integrity in dogs. *Reprod Domest Anim* 52(Suppl 2):310–15.
- Greco A, Meomartino L, Gnudi G, *et al.*, 2023. Imaging techniques in veterinary medicine. Part II: Computed tomography, magnetic resonance imaging, nuclear medicine. *Eur J Radiol Open* 10:100467; doi: 10.1016/j.ejro.2022.100467.
- Klansnöh U, Banlunara W and Chaisunirachon N, 2018. Computed tomographic contrast enhancement and tumor angiogenesis in canine oral tumors. *Thai J Vet Med* 48(4): 573–81.
- Kuhnt N, Harder LK, Nolte I, *et al.*, 2020. Computed tomographic features of the prostatic gland in neutered and intact dogs. *BMC Vet Res* 16(1):156; doi: 10.1186/s12917-020-02374-8.
- Lévy X, Nizański W, Von Heimendahl A, *et al.*, 2014. Diagnosis of common prostatic conditions in dogs: An update. *Reprod Domest Anim* 49:50–57.
- Leroy C, Conchou F, Layssol-Lamour C, *et al.*, 2013. Normal canine prostate gland: Repeatability, reproducibility, observer-dependent variability of ultrasonographic measurements of the prostate in healthy intact Beagles. *Anat Histol Embryol* 42(5):355–61.
- Mantzias G, 2020. Imaging of the male reproductive tract: Not so easy as it looks like. *Theriogenology* 150:490–97.
- Memor MA, 2007. Common causes of male dog infertility. *Theriogenology* 68(3): 322–28.
- Mukaratirwa S and Chitura T, 2007. Canine subclinical prostatic disease: Histological prevalence and validity of digital rectal examination as a screening test. *J S Afr Vet Assoc* 78:66–68.
- Nishikawa S, Miki M, Chigusa Y, *et al.*, 2023. Obstetric pelvimetry by three-dimensional computed tomography in non-pregnant Japanese women: A retrospective single-center study. *J Matern Fetal Neonatal Med* 36(1):2190444; doi: 10.1080/14767058.2023.2190444.
- Nizański W, Ochota M, Fontaine C, *et al.*, 2020. B-mode and doppler ultrasonographic findings of prostate gland and testes in dogs receiving Deslorelin acetate or Osaterone acetate. *Animals* 10:1–31.
- Pasikowska J, Hebel M, Nizański W, *et al.*, 2015. Computed tomography of the prostate gland in healthy intact dogs and dogs with benign prostatic hyperplasia. *Reprod Domest Anim* 50(5):776–83.
- Ruel Y, Barthez PY, Mailles A, *et al.*, 1998. Ultrasonographic evaluation of the prostate in healthy intact dogs. *Vet Radiol Ultrasound* 39(3):212–16.
- Russo M, Vignoli M and England GCW, 2012. B-mode and contrast-enhanced ultrasonographic findings in canine prostatic disorders. *Reprod Domest Anim* 47:238–42.
- Salonen HM, Åhlberg TM, Laitinen-Vapaavuori OM, *et al.*, 2022. CT measurement of prostate volume using OsiriX® viewer is reliable, repeatable, and not dependent on observer, CT protocol, or contrast enhancement in dogs. *Vet Radiol Ultrasound* 63(6):729–38.
- Smith J, 2008. Canine prostatic disease: A review of anatomy, pathology, diagnosis, and treatment. *Theriogenology* 70(3):375–83.
- Socha P, Zduńczyk S, Tobolski D, *et al.*, 2018. The effects of Osaterone acetate on clinical signs and prostate volume in dogs with benign prostatic hyperplasia. *Pol J Vet Sci* 21(4):797–802.
- Teske E, 2009. Urogenital cytology: Part I-prostatic diseases. In: *Proceedings of the 34th World Small Animal Veterinary Congress*, San Pablo, Brazil, P 5.
- Wilson EB, 1927. Probable inference, the law of succession, and statistical inference. *J Am Stat Assoc* 22(158):209–12.
- Zelli R, Orlandi R, Troisi A, *et al.*, 2013. Power and pulsed doppler evaluation of prostatic artery blood flow in normal and benign prostatic hyperplasia-affected dogs. *Reprod Domest Anim* 48(5):768–73.